Vehicle System Dynamics
Vol. 00, No. 00, Month 200x, 1–22

Realtime Multiple-Model Estimation of Center of Gravity Position in Automotive Vehicles

Selim Solmaz*†, Mehmet Akar ‡, Robert Shorten †, and Jens Kalkkuhl †

† Hamilton Institute, National University of Ireland-Maynooth, Co. Kildare, Ireland
‡ Dept. of Electrical and Electronics Engineering, Boğaziçi University, İstanbul, Turkey

(*Received 19 June 2006; In final form 2 July 2007*)

In this paper we present a methodology based on multiple models and switching for realtime estimation of center of gravity (CG) position in automotive vehicles. The method utilizes well-known simple linear vehicle models for lateral and roll dynamics and assumes the availability of standard stock automotive sensors. We illustrate the technique with numerical simulations as well as with measured sensor data from an SUV vehicle. We also compare our estimation results with traditional linear-least squares estimators to show the efficacy of our technique. Finally, we give a simple application example for implementing the idea in automotive vehicles as a switch for rollover controller activation.

Keywords: Center of Gravity Estimation, Rollover, Multiple Models, Switched Systems.

1 Introduction

Vehicle center of gravity (CG) position and inertial properties are of primal importance in the assessment of vehicle handling and performance characteristics as well as its accident behavior. Although automotive manufacturers often provide the measurement of these parameters, such information often pertains to an empty vehicle with known load distribution. Considering the fact that passenger, and/or load distribution in road vehicles can vary significantly, and sometimes even dangerously, it is difficult to overlook the change in the CG position and its consequences. While the importance of this is known on the handling behavior, automotive manufacturers usually employ robust active road-handling control strategies to account for the unknown and changing CG position; they simply design for the worst case scenario. Another common approach in the case of Sport Utility Vehicles (SUVs) is to intentionally design the vehicle heavier than usual by adding ballast in the undercarriage, which aims to lower the CG position while reducing the percent margin of the load variation and thus constraining the variation of the CG location. While such approaches are successful up to certain extent, they also come with obvious drawbacks; performance loss under normal driving conditions and reduced efficiency due to added weight.

Analysis of recent car accident data indicates that vehicles with a high center of gravity such as vans, trucks and SUVs are more prone to rollover accidents than others [1]. Moreover it is known that rollover accidents alone constitute only a small percentage of all car accidents, while they cause disproportionately high rates of fatalities [2]. According to [1] non-collision rollover occurred in only 2.3% of all vehicle crashes during 2004 in the USA, while it was responsible for a massive 10.6% fatality rate, rendering it to be the most dangerous type of accident. Again according to the same data, light trucks (pickups, vans, SUVs) were involved in nearly 70% of all the rollover accidents, with SUVs alone responsible for almost 35% of this total. Considering the fact that composition of the current automotive fleet consists of nearly 36% light trucks, minivans and SUVs [3] along with the recent increase in the popularity of SUVs worldwide, makes the rollover an important safety problem. As CG height is the most prominent factor in un-tripped rollover occurrence, this problem can greatly benefit from real-time CG position estimation capabilities. Such estimators can be used as a warning system to the driver or can conveniently be integrated into active road handling or rollover prevention controllers thus improving the overall vehicle and passenger safety.

* Corresponding author. Email: selim.solmaz@nuim.ie, Phone:+353 1 7086100, Fax: +353 1 7086269

Vehicle System Dynamics
ISSN 0042-3114 print / ISSN 1744-5159 online © 200x Taylor & Francis
http://www.tandf.co.uk/journals
DOI: 10.1080/00423110xxxxxxxxx

With this background in mind, and inspired by the Multiple Model Switching & Tuning (MMST) methodology [4–6], we present in this paper a multiple model and switching estimation algorithm based on simple linearized models and employing only standard stock automotive sensors [7]. While simplified linear models such as the single track model (i.e., bicycle model) and the roll plane model can represent the real vehicle behavior in a limited range of maneuvers and speeds, it is possible to use a multitude of these models and switch between them in an intelligent way in real time, to track the vehicle behavior accurately over the complete operating conditions. Moreover, proper parametrization of these models gives way to the rapid estimation of unknown and time-varying vehicle parameters through the selected models. Using the described multi-model approach in conjunction with linear roll plane models, one can estimate parameters such as the CG height and linear suspension parameters in relation to the rollover prevention problem. Through a similar implementation of multiple single track models one can also estimate parameters relevant to lateral dynamics control, such as the longitudinal CG position and linear tire stiffnesses. One of the benefits of this realtime estimation method is the fact that the method is immune to the nonlinear dependance of unknown vehicle parameters in the models as shall be apparent in the Section 2. During the derivation of the method in Section 3 we make no assumptions about the parameter vector having a linear dependance on the states. This is particularly important as the traditional linear regression type estimation techniques can not work in the case of non-linear parameter variations, which we shall demonstrate with numerical simulations in Section 3.

Recent publications related to automotive CG position measurement and estimation include that of Mango [8], where he described a method for accurately calculating the CG location based on portable wheel scales. His method requires external measurement equipment and is not intended for online measurement during regular driving conditions as it requires the vehicle to be stationary. In another recent article, Allen et al. [9] made a statistical analysis of vehicle inertial properties and CG positions as a function of weight, width, length and the height of the vehicle using the data for several existing stock cars. Although their analysis is useful in demonstrating the relationship between the several physical parameters of vehicles to their handling characteristics, their method can not be employed for realtime estimation purposes. There has been a number of recent publications about realtime estimation of vehicle parameters including the CG position. Vahidi et al. suggested a recursive linear least squares estimator with multiple forgetting factors in [10], for simultaneous estimation of the road grade and the vehicle mass in real time. Their algorithm took into account the different rates of change in both unknown parameters and incorporated different forgetting factors into the cost function of the recursive least squares algorithm. Their results are promising as demonstrated with both numerical and measured data, however their method assumes that vehicle model is linear in the unknown parameters, which is not the case for the method presented in the present paper as shall be clear in the sequel. In a recent thesis [11], a model based estimation method for road bank angle and CG height was suggested using extended Kalman filters. The presented results showed slow convergence rates in the estimations and the accuracy was questionable. In a recent European patent EP 0918003*B*1 [12] an alternative method for estimating the height of the CG in real-time was described. The method utilizes an estimated drive/brake slip of at least one wheel using the wheel speed sensors, which is then used to compute the instantaneous radius of the corresponding wheel. Using this information, the angle of the corresponding wheel axle with respect to the ground is computed and then used in an equation related to the lateral dynamics of the car to compute the CG height. Since there are no other publications other then the cited patent, the details and the limitations of this method is not known to the authors. As a last remark we note in the context of rollover prevention that all the methods suggested to date assume known CG height [2, 3, 13–19]. However as we have explained, it is particularly unrealistic to assume the CG height to be known, and this parameter can vary significantly with changing passenger and loading conditions especially in large passenger vehicles such as SUVs.

2 Vehicle modelling

In this section we present three different models for the lateral motion and roll plane dynamics of a car. We use linear models to simplify the implementation of the algorithm as well as to keep the required sensory information at a minimum level. All the models introduced here assume small angles and are valid when the steering input is small. Also, in the second order linear single track model described below, a weak relationship between the lateral and the roll dynamics is assumed, which is the case when the steering angle is small [20]. Note that the choice of the models here is a trade off between complexity and sensitivity to different operating conditions. The assumption

Table 1. Model parameters and definitions

Parameter	Description	Unit
m	Vehicle mass	$[kg]$
g	Gravitational constant	$[m/s^2]$
v_x	Vehicle longitudinal speed	$[m/s]$
δ	Steering angle	$[rad]$
J_{xx}	Roll moment of inertia of the sprung mass measured at the CG	$[kg \cdot m^2]$
J_{zz}	Yaw moment of inertia of the chassis measured at the CG	$[kg \cdot m^2]$
L	Axle separation, such that $L = l_v + l_h$	$[m]$
T	Track width	$[m]$
l_v	longitudinal CG position measured w.r.t. the front axle	$[m]$
l_h	longitudinal CG position measured w.r.t. the rear axle	$[m]$
h	CG height measured over the ground	$[m]$
c	suspension damping coefficient	$[kg \cdot m^2/s]$
k	suspension spring stiffness	$[kg \cdot m^2/s^2]$
C_v	linear tire stiffness coefficient for the front tire	$[N/rad]$
C_h	linear tire stiffness coefficient for the rear tire	$[N/rad]$
β	Sideslip angle at vehicle CG	$[rad]$
α_v	Sideslip angles at the front tire	$[rad]$
α_h	Sideslip angles at the rear tire	$[rad]$
ϕ	Roll angle measured at the roll center	$[rad]$
$\dot{\phi}$	Roll rate measured at the roll center	$[rad]$

of linear models and small angles in the following discussion is indeed a restrictive argument as the linear models are not dependable during extreme driving situations, where the knowledge of the unknown vehicle parameters is required most (e.g., for the deployment of a suitable control action). However, the method described in this paper is intended for estimating the unknown parameters during normal driving conditions and long before such extreme driving conditions occur. Use of more accurate nonlinear models that are valid both in the linear and the nonlinear regions of the vehicle operation envelope, in conjunction with the multiple model estimation algorithm that shall be described in sequel, is a straightforward future direction for this work.

Notation and definitions of the model parameters and variables are given in Table 1. In what follows we give three different dynamical equations of the motion of the car. For a through coverage of the derivations see [21], and [20]. Note that for simplicity, we assume in the following equations that, relative to the ground the sprung mass of the vehicle rolls about a horizontal axis along the centerline of the body.

2.1 *Single track model*

This two state linear model represents the horizontal dynamics of a car. It is also referred to as "the linear bicycle model" in the literature and is commonly used in automotive applications (see [22] for a good application example).

The model assumes constant velocity and small steering angle for linearization. See Fig. 1 for the representation and notation of the model. Notice that in this model we lump left and right tires into a single one at the axle centerline, hence the name "Bicycle Model" or "Single Track Model". We represent the horizontal dynamics in terms of the state variables β and $\dot{\psi}$. The lateral tire forces S_v, S_h for front and rear tires respectively, are represented as linear functions of the tire slip angles such that $S_v = C_v\alpha_v$, and $S_h = C_h\alpha_h$, where for small angles tire slip angles are given as follows

$$\alpha_v = \delta - \beta - \frac{l_v}{v_x}\dot{\psi} \tag{1}$$

$$\alpha_h = -\beta + \frac{l_h}{v_x}\dot{\psi}. \tag{2}$$

Also notice that since we assume small angles and constant longitudinal velocity, sideslip angle β satisfies the following;

$$\beta \approx \frac{v_y}{v_x}, \qquad \dot{\beta} \approx \frac{\dot{v}_y}{v_x}. \tag{3}$$

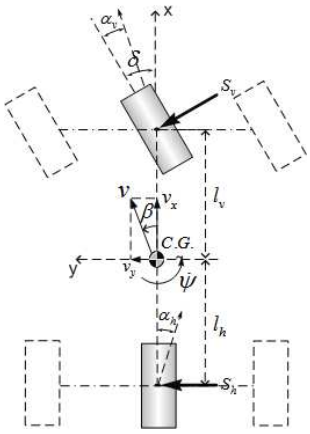

Figure 1. Linear bicycle model.

Using above relations and Newton's 2nd law of motion, one can get the following state space representation of the horizontal dynamics of the vehicle

$$\begin{bmatrix} \dot{\beta} \\ \ddot{\psi} \end{bmatrix} = \begin{bmatrix} -\frac{\sigma}{mv_x} & \frac{\rho}{mv_x^2} - 1 \\ \frac{\rho}{J_{zz}} & -\frac{\kappa}{J_{zz}v_x} \end{bmatrix} \cdot \begin{bmatrix} \beta \\ \dot{\psi} \end{bmatrix} + \begin{bmatrix} \frac{C_v}{mv_x} \\ \frac{C_v l_v}{J_{zz}} \end{bmatrix} \delta, \tag{4}$$

where the auxiliary parameters σ, ρ, and κ are defined as follows

$$\begin{aligned} \sigma &\triangleq C_v + C_h \\ \rho &\triangleq C_h l_h - C_v l_v \\ \kappa &\triangleq C_v l_v^2 + C_h l_h^2. \end{aligned} \tag{5}$$

We make use of this model mainly for the estimation of the uncertain model parameters C_v, C_h, l_v, l_h based on the multiple model structure. Note that although (4) is linear in the state variables, it is nonlinear with respect to unknown parameter variations, which is a factor limiting the use of traditional recursive estimation methods such as the linear least squares for the estimation of unknown parameters, as shall be demonstrated in the sequel.

Comment: In the version of the linear second-order single track model introduced here, the effect of the variations in longitudinal CG position to the variations in the effective yaw moment of inertia J_{zz} were ignored on the grounds that such changes are insignificant for small vehicles, where loading options are limited and the resulting changes in the inertia are quite small. For the sake of simplicity, parameters for a compact class vehicle were used in the simulations in this paper and therefore this assumption makes sense. However for larger vehicles such as busses and trucks the changes in yaw moment of inertia with changing longitudinal CG position can be quite significant and thus can not be ignored in the analysis.

Comment: It is important to note here also that the single track model assumes a weak coupling from the vertical (i.e., roll) dynamics onto the lateral. Therefore, there are no terms in (4) that reflect the effect of vertical dynamics, which is reasonable when the vehicle is operating in the linear regime at low levels of lateral acceleration [23]. However, the reverse argument is not true for the roll dynamics even under small angles assumption, since the roll motion is heavily influenced by the lateral dynamics via lateral acceleration, as shall be clear in the next subsection.

2.2 *Roll plane model*

We use the 2-state roll plane model described here for the realtime estimation of CG height h as well as the parameters of the suspension system k, c based on the multiple model switching method. This is the simplest model that captures the roll dynamics of the car and it is free from the effects of uncertainties originating from unknown tire stiffness parameters, which in turn makes it suitable for the estimation task.

Assuming all vehicle mass is sprung, effective linear torques exerted by the suspension system about the roll center are defined as follows

$$T_{spring} = k\,\phi, \tag{6}$$

$$T_{damper} = c\,\dot{\phi}, \tag{7}$$

where k, c denote the linear spring stiffness and damping coefficients respectively. Using these one can then apply a torque balance in the roll plane of the vehicle in terms of the effective suspension torques (see Fig. 2 for the notation of the roll plane model), and obtain the following relationship

$$J_{x_{eq}}\ddot{\phi} + c\dot{\phi} + k\phi = mh(a_y cos\phi + g sin\phi). \tag{8}$$

Note that for simplicity, it is assumed that, relative to the ground, the sprung mass rolls about a fixed horizontal roll axis which is along the centerline of the body and at ground level. In the last equation $J_{x_{eq}}$ denotes the equivalent roll moment of inertia derived using the parallel axis theorem of mechanics taking into account the CG height variation as described below

$$J_{x_{eq}} \triangleq J_{xx} + mh^2. \tag{9}$$

For small ϕ, we can approximate nonlinear terms in equation (8) as $cos\phi \approx 1$, $sin\phi \approx \phi$ and represent this equation as in the following state space form

$$\begin{bmatrix} \dot{\phi} \\ \ddot{\phi} \end{bmatrix} = \begin{bmatrix} 0 & 1 \\ -\frac{k-mgh}{J_{x_{eq}}} & -\frac{c}{J_{x_{eq}}} \end{bmatrix} \cdot \begin{bmatrix} \phi \\ \dot{\phi} \end{bmatrix} + \begin{bmatrix} 0 \\ \frac{mh}{J_{x_{eq}}} \end{bmatrix} a_y. \tag{10}$$

Note that at steady state one can calculate the CG height using a single model using the relationship

$$h = \frac{k\phi}{m(g\phi + a_y)}, \tag{11}$$

given that the roll angle ϕ, and the lateral acceleration a_y measurements as well as an accurate knowledge of the spring stiffness k are available. While former can be measured using suitable sensors, k is unknown and needs to be calculated depending on the specific maneuver and loading condition, and is effected by various other factors. As will be explained in Section 3, using the multiple model switching method we neither need the exact knowledge of the suspension parameters, nor steady state type excitation to get an accurate estimation of the CG height. As a final remark note that although (10) is linear in the state variables, again observe that it is nonlinear with respect to unknown parameter variations of k, c and h.

2.3 *Single track model with roll degree of freedom*

While we utilize the previous two models for the estimation task of the unknown vehicle parameters, we employ the linear bicycle model with roll degree of freedom described here, to generate the reference vehicle behavior. The model is the simplest model with coupled lateral and roll dynamics, which assumes that δ, ϕ, β are small and all vehicle mass is sprung. We can write the equations of motion for the single track model with the extended roll

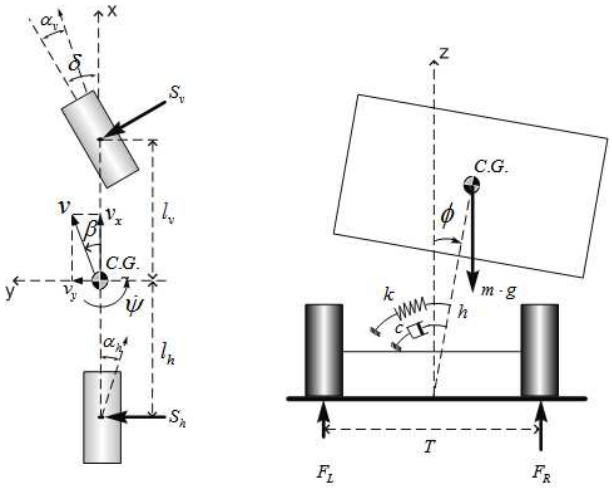

Figure 2. Linear bicycle model with roll degree of freedom.

degree of freedom as follows

$$\dot{x} = \begin{bmatrix} -\frac{\sigma}{mv_x}\frac{J_{xeq}}{J_{xx}} & \frac{\rho}{mv_x^2}\frac{J_{xeq}}{J_{xx}} - 1 & -\frac{hc}{J_{xx}v_x} & \frac{h(mgh-k)}{J_{xx}v_x} \\ \frac{\rho}{J_{zz}} & -\frac{\kappa}{J_{zz}v_x} & 0 & 0 \\ -\frac{h\sigma}{J_{xx}} & \frac{h\rho}{v_xJ_{xx}} & -\frac{c}{J_{xx}} & \frac{mgh-k}{J_{xx}} \\ 0 & 0 & 1 & 0 \end{bmatrix} x + \begin{bmatrix} \frac{C_v}{mv_x}\frac{J_{xeq}}{J_{xx}} \\ \frac{C_vl_v}{J_{zz}} \\ \frac{hC_v}{J_{xx}} \\ 0 \end{bmatrix} \delta, \tag{12}$$

where $x = \begin{bmatrix} \beta & \dot{\psi} & \dot{\phi} & \phi \end{bmatrix}^T$ is the state vector. Representative state responses of this model to a step steering input are shown in Fig. 3 below, where the steering magnitude was 30° with a steering ratio of 1 : 18, and the vehicle velocity during the simulation was $v_x = 30m/s$.

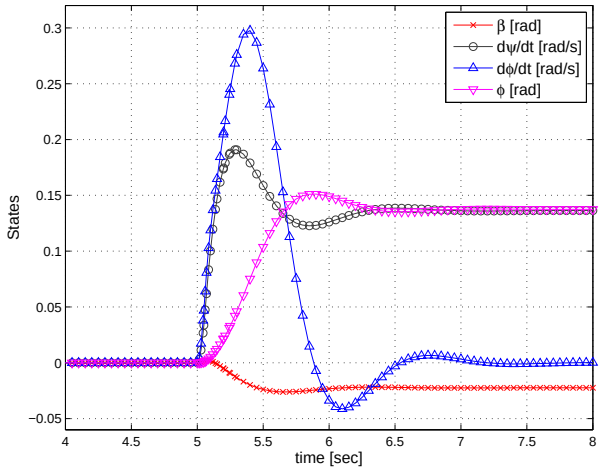

Figure 3. State responses of the single track model with roll degree of freedom to a step steering input ($v_x = 30m/s$, $\delta = \frac{30}{18}^\circ$.)

2.4 *Sensors and vehicle parameters*

In this subsection we describe the configuration of sensors, and summarize the list of the assumptions on the known and estimated vehicle parameters.

2.5.1 Sensors: In this paper we assume the availability of lateral acceleration a_y, yaw rate $\dot{\psi}$, velocity v_x and the steering angle δ measurements which are available as part of the standard sensor packs found in modern cars that are commonly utilized for lateral and yaw dynamics control implementations such as the ESP (Electronic Stability Program) [22], [24]. Moreover, a measurement or an estimation of the vehicle roll angle is required for the implementation in this paper, which can be obtained through spring displacement sensors (displacement transducers) found in vehicles with active suspension systems such as the ABC (Active Body Control).

Comment: The analysis given in this paper does not necessarily require the use of particular type of sensor to obtain the roll angle information: gyroscopic roll rate sensors, or any other suitable set of sensors can be utilized for computing the roll angle.

2.5.2 Parameters: We assume that vehicle mass m is known, which can be estimated as part of the braking system (see for example [10]), yet this is outside scope of this paper. Furthermore C_v, C_h, l_v, k, c and h are all assumed be **unknown** parameters of the vehicle and are estimated through the multiple model switching algorithm. We further assume that these parameters vary within certain closed intervals $C_v \in \mathscr{C}_v$, $C_h \in \mathscr{C}_h$, $l_v \in \mathscr{L}_v$, $c \in \mathscr{C}$, $k \in \mathscr{K}$ and $h \in \mathscr{H}$, and these intervals can be found via accurate numerical simulations as well as field tests. The number of models necessary to estimate these parameters relates to the size of the interval and the accuracy demand on the estimation, as shall be explained in the following section.

Comment: It is possible to extend the estimation scheme described in the next section to include the unknown and time-varying vehicle mass. However, as there are alternative and dependable methods for estimating the vehicle mass [10], as well as for the ease of exposition of the method described here, we omitted this parameter in the following discussion.

3 Vehicle parameter identification through multiple models & switching

While the conventional approach to parameter estimation is to employ a well-established linear least square type identification technique, such methods are susceptible to loss of identifiability due to feedback [25], [26] as is the case for the estimation problem described here. Also, the linear models introduced in Section 2 are nonlinear in the unknown vehicle parameters further complicating the formulation of the estimation problem using the traditional approaches. Although linear regression techniques typically converge quickly, they require measurement signals that are persistently exciting [25], [27]. For our problem this would mean to impose some specific maneuver requirements on the driver input such that all the modes of excitation are covered and a dependable estimation of the unknown parameters could be made. Such a demand on the driver input would not only be unrealistic but also unreliable. Thus there is a need for a different approach for the parameter identification task, which imposes no restriction on the driver input, has fast convergence rates and requires minimum additional output information (sensors). Here we introduce a multiple model switching algorithm [7] to identify unknown vehicle parameters rapidly in real-time. The method achieves this, in part, as a result of the fact that the model space representing the parameter uncertainty is bounded, and includes only the feasible parameters of the vehicle. This restricts infeasible estimations in cases when sensor signal are not persistently excited, and where the standard estimation methods such the recursive linear least squares are destined to fail. Although we have no theoretical proof that the multiple model estimation algorithm is more immune to persistence of excitation issues, our numerical analysis shows that this is the case, at least as compared to the standard recursive least square algorithm. An extensive theoretical analysis of this is a future research direction for this work.

A natural approach here would be to setup the multiple estimation models using (12), which in this setup would imply that there is no modelling error. However in this case, the resulting parameter space would be too complex to handle. Instead we take a modular approach of decoupling the vehicle dynamics into subsystems by assuming a weak relationship from the roll dynamics onto the lateral. In the following two subsections we present our methodology and give numerical simulation results corresponding to the decoupled identification algorithms, which are then compared to recursive least squares based estimations.

3.1 *Online identification of longitudinal CG location and tire stiffness parameters*

The multiple model switching identification algorithm to estimate longitudinal CG location l_v and tire stiffness parameters C_v, C_h makes use of the lateral dynamics model given in (4). The method assumes that each unknown parameter belongs to a closed interval such that $C_v \in \mathscr{C}_v$, $C_h \in \mathscr{C}_h$, and $l_v \in \mathscr{L}_v$. These intervals are divided into certain number of grid points and they can be represented as $\mathscr{C}_v = \{C_{v_1}, C_{v_2}, C_{v_3}, \ldots, C_{v_p}\}$, $\mathscr{C}_h = \{C_{h_1}, C_{h_2}, C_{h_3}, \ldots, C_{h_q}\}$, and $\mathscr{L}_v = \{l_{v_1}, l_{v_2}, l_{v_3}, \ldots, l_{v_r}\}$ with dimensions p, q and r respectively.

Comment: There is a trade-off between the choice of the number of grid points in the parameter space and the numerical complexity, which is a design consideration depending on the accuracy demand from the estimation and the available computational resources for the specific problem under consideration.

With these in mind we form $n = p \times q \times r$ different models corresponding to the cross combinations of the grid points in the parameter space. Utilizing (4), the equations of motion corresponding to each model can be represented as

$$\begin{bmatrix} \dot{\beta}_i \\ \ddot{\psi}_i \end{bmatrix} = \begin{bmatrix} -\frac{\sigma_i}{mv_x} & \frac{\rho_i}{mv_x^2} - 1 \\ \frac{\rho_i}{J_{zz}} & -\frac{\kappa_i}{J_{zz}v_x} \end{bmatrix} \cdot \begin{bmatrix} \beta_i \\ \dot{\psi}_i \end{bmatrix} + \begin{bmatrix} \frac{(C_v)_i}{mv_x} \\ \frac{(C_v)_i l_{v_i}}{J_{zz}} \end{bmatrix} \delta, \tag{13}$$

where $i = 1, 2, \ldots, n$ denotes the model number. We assume that all models have zero initial conditions such that $\beta_i(0) = 0$, and $\dot{\psi}_i(0) = 0$, for $i = 1, 2, \ldots, n$. Furthermore, each model is driven by the same inputs δ and v_x as depicted in Fig. 4, measurements of which are assumed to be provided by suitable set of sensors. In order to select

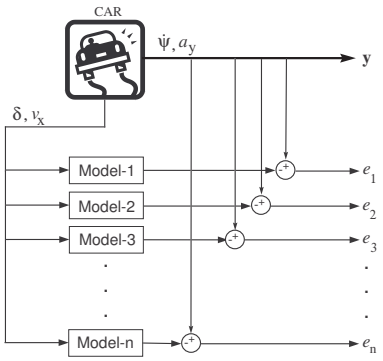

Figure 4. Multiple Model System Identification Algorithm.

the model with the correct parametrization we look at the difference between the model and the plant outputs. The identification error e_i corresponding i^{th} model is defined as

$$e_i = y_{plant} - (y_{model})_i, \tag{14}$$

where y denotes the model or the plant output. In this implementation of the algorithm the output to be utilized is $y = [a_y, \dot{\psi}]$, and it is further assumed that the measurement of these are available for the vehicle. Thus we can represent the identification error for the i^{th} model as follows

$$e_i(t) = \begin{bmatrix} a_y(t) - a_{y,i}(t) \\ \dot{\psi}(t) - \dot{\psi}_i(t) \end{bmatrix}, \quad i = 1, 2, \ldots, n. \tag{15}$$

Note here that $a_y(t)$ and $\dot{\psi}(t)$ are the respective plant lateral acceleration and yaw rate output measurements obtained from the sensors, while $\dot{\psi}_i(t)$ is obtained from the second state of the i^{th} single track model given in (13), and

corresponding $a_{y,i}(t)$ is calculated using the following function of the states at every instant

$$a_{y,i} = v_x(\dot{\psi}_i + \dot{\beta}_i) = -\frac{\sigma_i}{m}\beta_i + \frac{\rho_i}{mv_x}\dot{\psi}_i + \frac{(C_v)_i}{m}\delta. \tag{16}$$

By utilizing the identification errors it is possible to switch and choose a model that has the minimum distance to the plant outputs. Although control design is outside the scope of the current paper, using a model that has the closest outputs to those of the plant is likely to yield the best feedback performance. In other words a small identification error leads to a small tracking error [6], which, in the sense of adaptive control, is based on the principle of certainty equivalence from tuning to switching [28]. Control design implementation of the algorithm shall be explored in our future work.

Based on empirical observations, the choice of the switching index should include both instantaneous and steady-state measures in order to reliably determine the identification models representing the plant at all instants. While there exist many such indices, we utilize the cost function J_i corresponding to the i^{th} identification error as given below, which is inspired by the quadratic cost optimization techniques and was originally suggested by Narendra et al. in [4–6] as a switching scheme

$$J_i(t) = \alpha||e_i(t)|| + \beta\int_0^t e^{-\lambda(t-\tau)}||e_i(\tau)||d\tau. \tag{17}$$

In this cost function $\alpha > 0$, and $\beta > 0$ are free design parameters controlling the relative weights given to transient and steady state measures respectively, whereas $\lambda \geq 0$ is the forgetting factor. As will be demonstrated in the sequel, switching based on (17) with nonzero combinations of α, β gives better results then using just the transient measures, e.g. $J_i(t) = e_i(t)^2$, or the steady-state measures, e.g. $J_i(t) = \int_0^t ||e_i(\tau)||d\tau$ alone. This is illustrated in Fig. 5, where a comparison of the switching rule based on transient ($\alpha = 1, \beta = 0$), steady-state ($\alpha = 0, \beta = 1$) and combined ($\alpha = 0.2, \beta = 0.8$) output error dynamics is presented during the estimation of the longitudinal position of CG, where the true value of the reference vehicle is $1.2m$. It is obvious from the figure that the switching based on just the transient measures causes an undesirable chattering, while switching based only on the steady state measures has slower response in the estimations. For the details of the simulation see the following subsection on numerical analysis. Note that it is possible to use other type of cost functions depending on the specific estimation

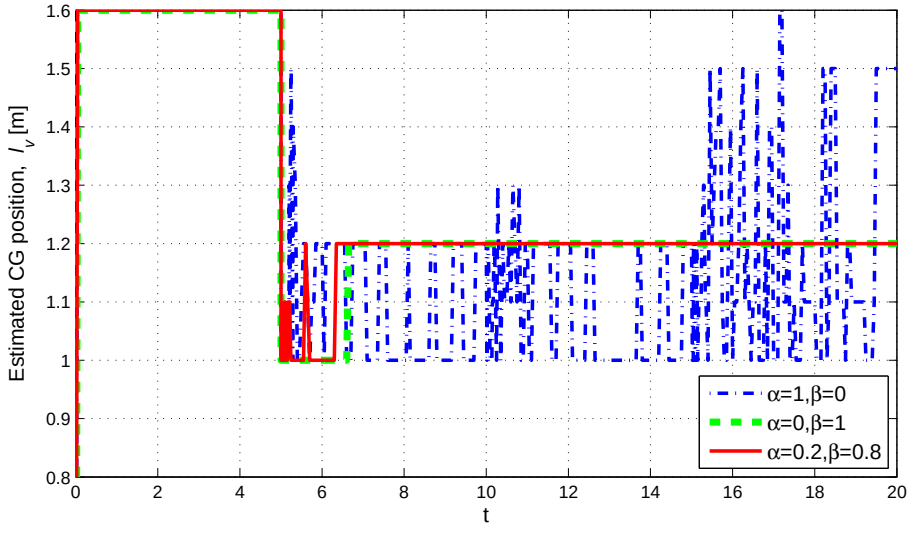

Figure 5. Comparison of switching based on transient, steady-state and combined output error dynamics during the estimation of longitudinal CG position.

requirements from the problem at hand. Here we selected the model with the least cumulative identification error

Table 2. Reference Model Parameters

parameter	value	unit
m	1300	$[kg]$
g	9.81	$[m/s^2]$
v_x	30	$[m/s]$
δ_{peak}	$30 \cdot \frac{1}{18}$	$[deg]$
J_{xx}	400	$[kg \cdot m^2]$
J_{zz}	1200	$[kg \cdot m^2]$
l_v	**1.2**	$[m]$
l_h	1.3	$[m]$
L	2.5	$[m]$
h	**0.7**	$[m]$
c	5000	$[kg \cdot m^2/s]$
k	36000	$[kg \cdot m^2/s^2]$
C_v	60000	$[N/rad]$
C_h	90000	$[N/rad]$

according to (17) using

$$i^\star = \arg \min_{i=1,\ldots,N} J_i(t). \tag{18}$$

Within the parameter space described by $\mathscr{C}_v, \mathscr{C}_h$ and $\mathscr{L}_v$, selected model $i^\star$ and the corresponding model parameters $C_v^\star, C_h^\star$ and $l_v^\star$ have the minimum cumulative distance to the parameters of the plant.

Comment: As a rule of thumb based on our numerical experimentation, choosing $0.9 \leq \beta \leq 1$ and $0 < \alpha \leq 0.1$ for this problem gave the best estimation results in conjunction with the multiple model switched estimation algorithm. Also, the forgetting factor λ becomes important if the plant undergoes rapid switches; as this is not the case when CG position variation is considered, we set $\lambda = 0$ in the following discussion.

Numerical analysis: In the following figures we present the estimation results for the algorithm based on simulated sensor signals generated by the vehicle model (12). The model parameters used are given in Table 2. The maneuver was conducted at $108 km/h$, and as seen in Fig. 6 the maneuver tested was an obstacle avoidance maneuver commonly known as the elk-test, with a peak magnitude of 30° at the steering wheel (the steering ratio is 1/18 between the tires and the steering wheel). The model space consisted of 140 models in total. The uniformly distributed parameter space were selected as $\mathscr{C}_v = [50000, 80000]$ with intervals of 10000, $\mathscr{C}_h = [60000, 100000]$ with intervals of 10000 corresponding to the range of tire stiffness parameters, and $\mathscr{L}_v = [1, 1.6]$ with intervals of 0.1 corresponding to the space of possible longitudinal CG positions. For this numerical example the free design parameters for the cost function were set as $\alpha = 0.05$ and $\beta = 1$, while the forgetting factor λ was chosen to be 0.

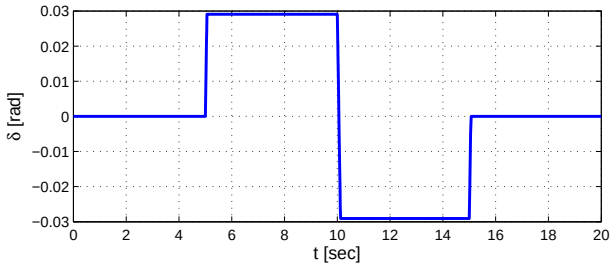

Figure 6. Steering input.

In Fig. 7 the corresponding simulated sensor data and selected model outputs are compared. The discontinuous jumps in the model outputs are the result of the switching between the models. In Fig. 8 the longitudinal CG position estimation is presented, where switching is more obvious. It is observed that based on the simulated measurement data, the multiple model switching algorithm successfully estimated the longitudinal CG location to be $1.2m$, precisely matching the reference model. Similarly in Fig. 9 the estimations for the front and rear tire stiffnesses with

exact model match are presented. The algorithm successfully estimated the front tire stiffness C_v as 60000 and rear tire stiffness C_h as 90000, which are the exact parameters of the reference model. Finally in Fig. 10 reference model sideslip angle β is compared with respect to that of the selected model which shows good agreement. For all practical means, the estimation result presented here is within sufficient tolerances for use in automotive control applications, particularly for adaptive lateral dynamics control problem.

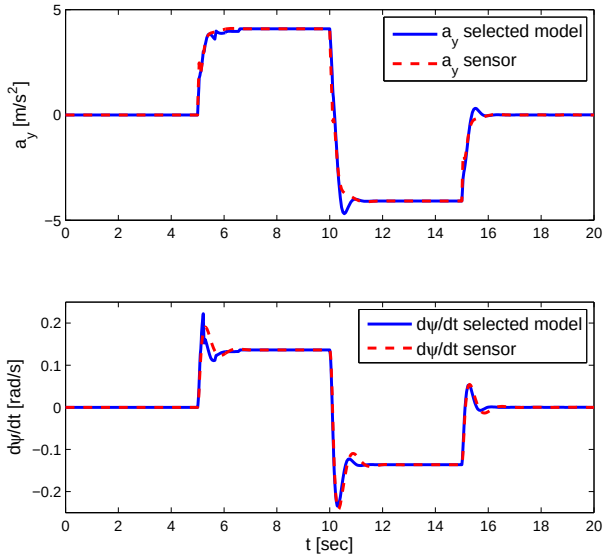

Figure 7. Sensor and the selected model output comparison for the longitudinal CG position estimation.

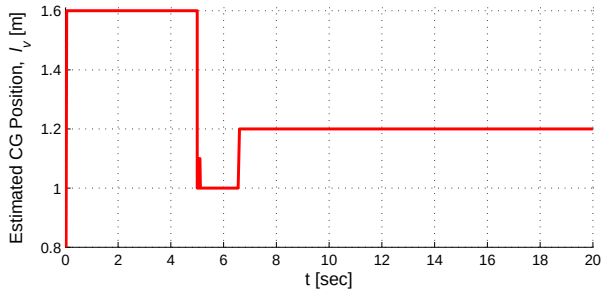

Figure 8. Longitudinal CG position estimation with exact match.

Comment: A theoretical issue related to switching between the identification models based on the cost function (17) of the identification errors is due to fact that it is difficult to guarantee one-to-one correspondence between the distance (or error) in the output space and the distance in the parameter space at every instant. This can be demonstrated by defining a normalized parameter error corresponding to the i^{th} identification model as follows

$$\varepsilon_i = \sqrt{\left(1-\frac{(l_v)_i}{l_{v,p}}\right)^2 + \left(1-\frac{(C_v)_i}{C_{v,p}}\right)^2 + \left(1-\frac{(C_h)_i}{C_{h,p}}\right)^2}, \quad i = 1,2,...,n, \tag{19}$$

where $l_{v,p}, C_{v,p}$, and $C_{h,p}$, denote the real parameters of the vehicle that we are trying to estimate. Note that for a given identification model, the normalized parameter error defined above is constant. At a given time instant t, the relationship between ε_i and $J_i(t)$ can be shown by comparing their variations across the model space (i.e.,

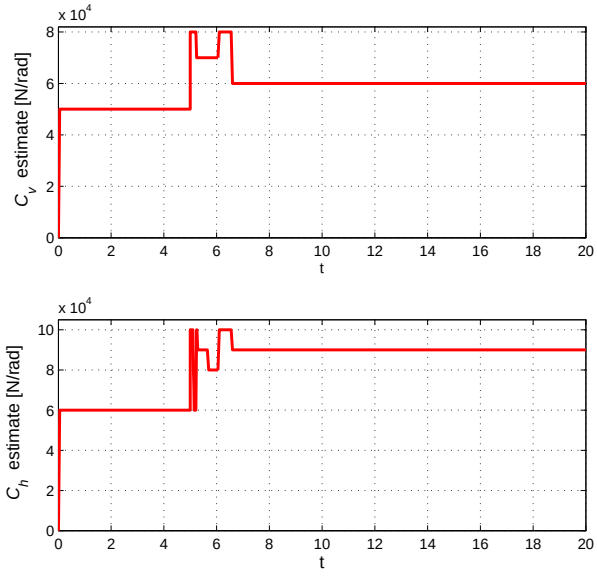

Figure 9. Estimation of the front and rear linear tire stiffness with exact model match.

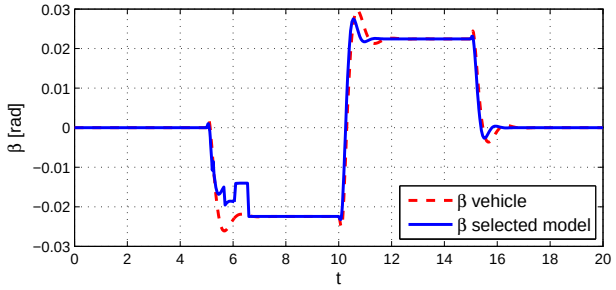

Figure 10. Comparison of the sideslip angles β for the vehicle and the selected models during the maneuver.

models corresponding to all combinations of the parameters). This is given in Fig. 11 at an instant shortly after the initiation of the maneuver $(t = 5.25sec)$ for the 140 models used in the numerical simulation, and the result clearly demonstrates the problem with the non-correspondence between output and parameter spaces at this instant, where transient dynamics are dominant. In Fig. 12 however, the time history of the normalized parameter error corresponding to the selected model at each instant during the estimation is shown, where it is observed that the parameter error goes to zero. This can be attributed to the fact that as the steady-state dynamics start to dominate, the cost functions $J_i(t)$ corresponding models with large parameter errors grow much faster than those with small parameter errors, yielding the desired estimation result. To the best of the authors' knowledge, determination of a cost function of the output errors that has a one-to-one correspondence in the parameter space at every instant, is still an open question in this framework.

3.2 *Online identification of CG height and suspension system parameters*

In this subsection we present the multiple model switching algorithm to estimate CG height h along with the linear suspension parameters k, c based on the roll-plane model (10). Similarly, we assume that each unknown parameter belongs to a closed interval such that $h \in \mathscr{H}$, $k \in \mathscr{K}$, and $c \in \mathscr{C}$. These intervals are divided into sufficient number of grid points and they can be represented as $\mathscr{H} = \{h_1, h_2, h_3, \ldots, h_p\}$, $\mathscr{K} = \{k_1, k_2, k_3, \ldots, k_q\}$, and $\mathscr{C} = \{c_1, c_2, c_3, \ldots, c_r\}$ with dimensions p, q and r respectively. We then form $n = p \times q \times r$ different models corresponding to the cross combinations of the grid points in the parameter space. Utilizing (10) the equations of

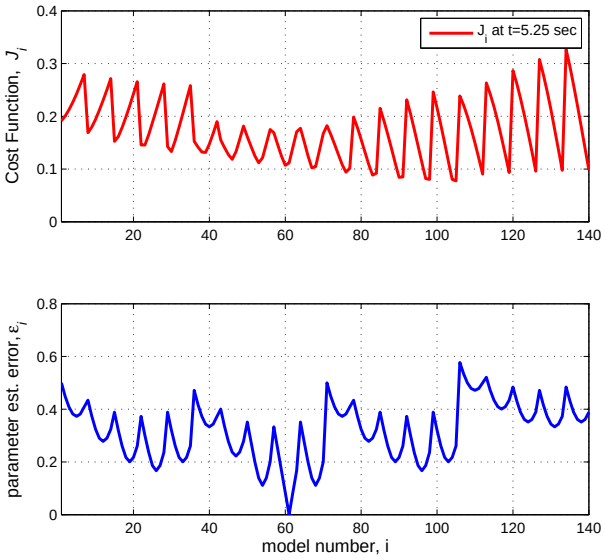

Figure 11. Variation of the cost functions J_i across the model space at an instant $(t = 5.25sec)$ shortly after the initiation of the maneuver and compared to the normalized parameter error ε_i for the numerical example.

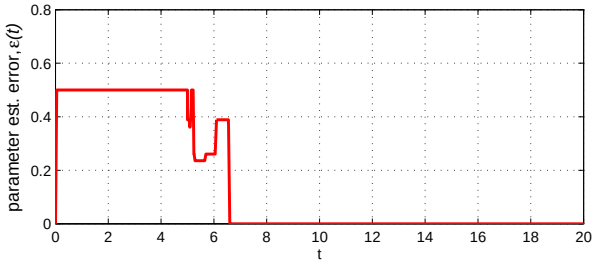

Figure 12. Time history of the normalized parameter error $\varepsilon(t)$ of the selected model during the simulation.

motion corresponding to each model can be represented as

$$\begin{bmatrix} \dot{\phi}_i \\ \ddot{\phi}_i \end{bmatrix} = \begin{bmatrix} 0 & 1 \\ -\frac{k_i - mgh_i}{J_{x_{eq},i}} & -\frac{c_i}{J_{x_{eq},i}} \end{bmatrix} \cdot \begin{bmatrix} \phi_i \\ \dot{\phi}_i \end{bmatrix} + \begin{bmatrix} 0 \\ \frac{mh_i}{J_{x_{eq},i}} \end{bmatrix} a_y, \tag{20}$$

where $i = 1,2,\ldots,n$ denotes the model number. We assume that all models have zero initial conditions such that $\phi_i(0) = 0$, and $\dot{\phi}_i(0) = 0$, for $i = 1,2,\ldots,n$. Similar to what is shown in Fig. 4, every model is driven by the same input a_y, which is measured. According to (14) we again calculate identification errors e_i, however this time the plant and model outputs to compare are the roll angles, as follows

$$e_i(t) = \phi(t) - \phi_i(t), \quad i = 1,2,\ldots,n. \tag{21}$$

Note that one can also include the roll rate $\dot{\phi}$ measurement if available, in the output vector. However, the influence of $\dot{\phi}$ on the estimation results for the CG height was relatively insignificant as compared to the roll angle ϕ, thus was omitted here. This is also in accordance with our assumption of no additional sensors to the available ones.

Now one can compute cost functions (17) corresponding to each identification error. Switching among the models based on (18) yields the one with the minimum cumulative identification error and the selected $k^\star, c^\star$ and $h^\star$ represent the plant in the parameter space described by $\mathscr{K}$, $\mathscr{C}$ and $\mathscr{H}$ respectively.

Numerical analysis: Here we present the CG height estimation results for the simulated measurement data

described in the previous subsection. The model space consisted of 240 models in total. The uniformly distributed parameter space were selected as $\mathscr{K} = [30000, 40000]$ with intervals of 2000, $\mathscr{C} = [4000, 6000]$ with intervals of 500 corresponding to the parameter space for suspension parameters, and $\mathscr{H} = [0.5, 0.85]$ with intervals of 0.05 corresponding to the range of possible CG heights. For this numerical example the free design parameters for the cost function were set as $\alpha = 0.01$ and $\beta = 1$, while the forgetting factor λ was chosen to be 0.

In Fig. 13 sensor and the switched model outputs are compared whereas in Fig. 14 the CG height estimation results are shown. Based on the results, we again observe that the multiple model switching algorithm successfully estimated the CG height to be 0.7 *m*, precisely matching the reference vehicle data. Finally in Fig. 15 the corresponding estimations of the suspension parameters are presented. The linear torsional spring stiffness k was estimated as 36000 exactly matching that of the reference vehicle model, while the roll damping coefficient c was estimated to be 6000 with a 20% estimation error.

Comment: The 20% estimation error in the damping coefficient can be attributed to the specific expression chosen for the model identification errors $e_i(t)$ given in (21), which is based on the roll angle measurements alone. As apparent from the expression for roll dynamics as described by (8), the damping coefficient c relates to the roll rate of the vehicle. Since we do not consider the roll rate estimation error in (21), this results in some expected estimation offset in c.

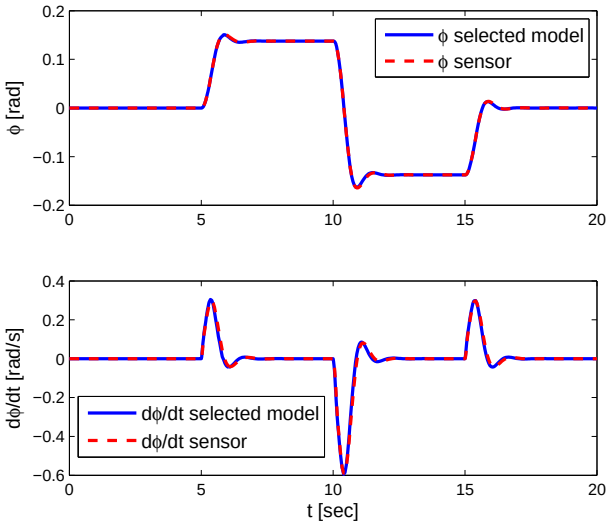

Figure 13. Sensor and the selected model output comparison for the CG height estimation.

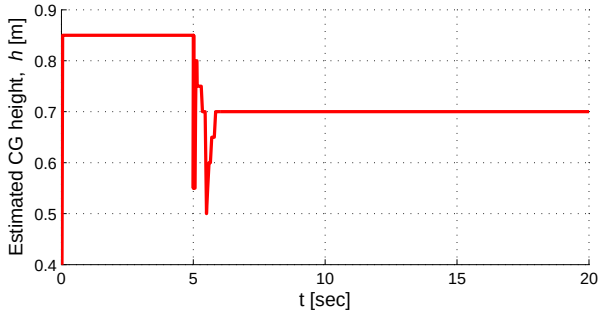

Figure 14. CG height estimation with exact match.

Despite the estimation offset in the roll damping coefficient, the suggested algorithm was successful in providing a fast and accurate estimation of the CG height, which is the main concern in this discussion. Therefore, for all

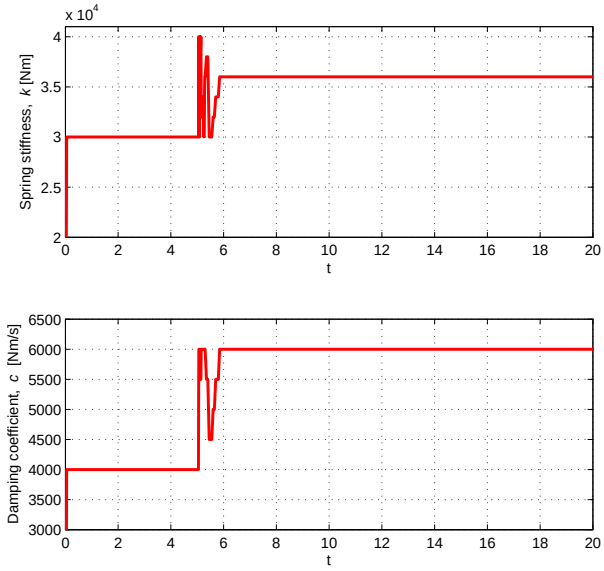

Figure 15. Estimation of the suspension parameters k, and c.

practical means, the method described here is suitable for use in active automotive handling control systems, particularly in rollover mitigation control applications.

Comment: For the CG height estimation algorithm, the road bank angle (road superelevation) was not considered. When a measurement or an estimation of this parameter is provided, (where there is vast number of literature on this topic), the analysis presented in this section can be extended and applied without much modification.

Comment: In the numerical simulations presented in this and the previous subsection, the parameter sets $\mathscr{C}_v, \mathscr{C}_h, \mathscr{L}, \mathscr{K}, \mathscr{C}, \mathscr{H}$ representing the uncertainty in the system were constructed such that the grid points include the unknown plant parameters of the reference model. When the parameter sets do not contain the exact model parametrization then the method can only guarantee that the selected model outputs match the sensor measurements, yet the selected model may not necessarily have the closest distance in the parameter space to the plant. It is however possible to include a vast amount of grid points to resolve this issue, which may be computationally difficult to implement in automotive applications. Alternatively, parameter adaptation rules or redistribution of the parameter space can be implemented to provide the exact model match, which we shall investigate as a continuation of this work. For automotive applications it is reasonable to utilize a uniform parametrization as described in the preceding sections as the loading conditions are usually restricted and can be represented with a small number of parameter sets.

3.3 *Estimation of CG position using recursive least squares*

In order to compare the quality of estimations described in the preceding subsections thus far, we now introduce a conventional method for estimating the CG position based on recursive linear least squares method. Although there exists other, perhaps more suitable methods, we chose this one since it is easier to implement. We first define the estimation method for a generic scalar system given by

$$y(t) = \xi^T(t)\theta + \varepsilon(t), \tag{22}$$

where $y(t)$ is the measurement corrupted by noise, $\varepsilon(t)$ is the measurement error, $\theta = [\theta_1, \theta_2, ..., \theta_N]^T$ is the unknown parameter vector, and $\xi = [\xi_1, \xi_2, ..., \xi_N]^T$ is the known regression vector. Using this system and denoting

$\hat{\theta}(t)$ as the estimation of the unknown parameter vector θ at time t, we can give the recursive least squares method as follows

$$\begin{aligned} \kappa(t) &= P(t-1)\xi(t)[1+\xi(t)^T P(t-1)\xi(t)]^{-1} \\ P(t) &= [I-\kappa(t)\xi(t)^T]P(t-1) \\ \hat{\theta}(t) &= \hat{\theta}(t-1)+\kappa(t)[y(t)-\xi(t)^T\hat{\theta}(t-1)], \end{aligned} \tag{23}$$

where $P(t)$ is error the covariance matrix, and $\kappa(t)$ is the gain vector. Initial value for the covariance matrix is selected as $P(0)=\alpha I$, where I is the identity matrix and α is a large scalar constant. Notice that the estimation $\hat{\theta}(t)$ is calculated based on the previous estimation $\hat{\theta}(t-1)$ and the current measurements only. For a detailed derivation of these equations see [26].

We give the implementation of CG height estimation based on this method and making use of (8). In this implementation we assumed availability of the measurements for $\phi,\dot{\phi},\ddot{\phi}$ as well as a_y, where simulated sensor signals are generated by the single track model with roll degree of freedom given in (12). We first denote the measurement vector as follows

$$a_y^{meas} = a_y cos\phi + gsin\phi. \tag{24}$$

As our reference model (12) is linear in the states as a result of the small angles assumption, for consistency, we can also express the measurement vector a_y^{meas} using the same assumption as follows

$$a_y^{meas} = a_y + g\phi. \tag{25}$$

Making use of (25) therefore, one can express the roll dynamics (8) as

$$y(t) = a_y^{meas} = \frac{1}{mh}[J_{x_{eq}}\ddot{\phi} + c\dot{\phi} + k\phi]. \tag{26}$$

Notice here that there is a nonlinear coupling between the measurement variable $y(t)$ and the state variables $\dot{\phi}$ and ϕ, which is likely to induce errors in the estimations as the linearity assumption of the least squares do not hold. For this type of coupled estimation problems more complicated instrumental-variable type methods are employed [25]. For demonstration purposes however we proceed with the recursive least squares method to present the shortcomings of this method as compared to ours. Keeping these in mind, we further denote the regression and the unknown parameter vectors respectively as follows

$$\xi = \begin{bmatrix} \ddot{\phi} & \dot{\phi} & \phi \end{bmatrix}^T, \tag{27}$$

$$\theta = \begin{bmatrix} \theta_1 & \theta_2 & \theta_3 \end{bmatrix}^T, \tag{28}$$

where $\theta_1 = \frac{J_{xeq}}{mh}$, $\theta_2 = \frac{c}{mh}$, and $\theta_3 = \frac{k}{mh}$. One can now use the recursive formulas (23) to compute $\hat{\theta}$ that minimizes the square of the cumulative measurement error. Based on the estimated parameters $\hat{\theta}$, the CG height can then be calculated from the roots of the polynomial below

$$mh^2 - m\theta_1 h + J_{xx} = 0. \tag{29}$$

As there are two roots of this polynomial, it is uncertain which one is closer to the real unknown parameter. In order to be conservative we always selected the larger root in the computations. The estimation result using this algorithm and employing the reference vehicle data introduced in the preceding section is given in Fig. 16 as compared to the multiple model based estimation. As it is apparent from the figure, even though least squares method utilized a vast amount of sensory information (some of which are unmeasurable using the standard vehicle sensor equipment), the corresponding estimation has an undesirable bias and its convergence rate is slower than the multi-model based

estimation. This clearly demonstrates the efficacy of our estimation technique over the traditional least squares approach for this specific problem. There are, however more sophisticated, and perhaps more suitable recursive estimation methods such as the instrumental-variable predictors or the least squares algorithm with multiple resetting as described in [10]. More extensive comparison of these alternative methods with the multiple model switching algorithm will be conducted in a future extension of the current paper.

Comment: One of the advantages of the multiple model based estimation over the recursive least squares method is due to the fact that the former limits the possible set of solutions of the estimation problem by using a finite number of models and performs, basically, hypothesis testing. This inherently eliminates infeasible solutions. However, in recursive least squares method it is possible to get numerical problems due to dynamics that are not stimulated persistently (for an example of this, see [20] Section 7.2).

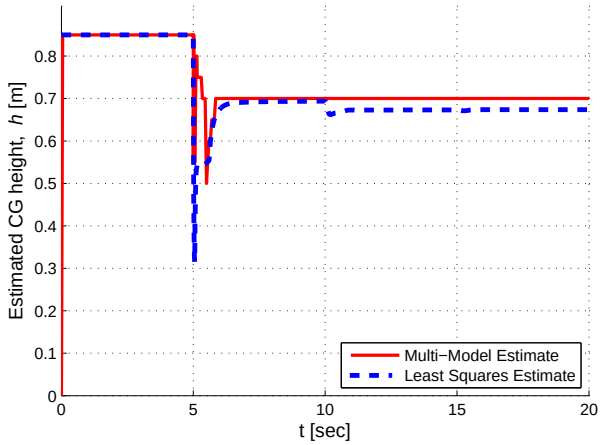

Figure 16. CG height estimation based on recursive least squares method as compared to the multiple model switching approach.

4 Preliminary evaluation of the CG position estimation algorithm with off-line sensor measurements

In this section we present the results of preliminary tests conducted with sensor measurement data obtained from an industrial partner without disclosing the type and make of the test vehicle. The mass and inertia properties of the vehicle were specified as $m = 3062kg$, $J_{zz} = 4892kg/m^2$, and $J_{xx} = 1174kg/m^2$. The velocity and steering angle corresponding to the measurement are shown in Fig. 17. It is important to note here that no feedback control systems were active during the measurements.

For the estimation of the longitudinal CG position, the parameter space consisted 180 models with the grid points selected as $\mathscr{L}_v = [1.3, 1.4, 1.425, 1.45, 1.475, 1.5, 1.525, 1.55, 1.6]$, $Cv = 1000 \cdot [80, 100, 120, 140]$, and $\mathscr{C}_h = 1000 \cdot [120, 140, 160, 180, 200]$. For this numerical example the free design parameters for the cost function were set as $\alpha = 0.01$ and $\beta = 0.99$, while the forgetting factor λ was chosen to be 0. Comparison of the measured lateral acceleration and yaw rate of the vehicle to that of the multiple model algorithm is shown in Fig. 18. Note here that there is a noticeable bias in the yaw rate measurement. Corresponding unknown parameter estimates of l_v, C_v and C_h are shown in Fig. 19.

The results of the estimation of CG height using multiple roll plane models using the measurement data are shown in Fig. 20 and Fig. 21. In this estimation, the model space consisted of 275 models in total with parameter grid points set as $\mathscr{K} = 1000 \cdot [190, 195, 200, 205, 210]$, $\mathscr{C} = 100 \cdot [30, 40, 50, 60, 70]$ and $\mathscr{H} = [0.55, 0.6, 0.65, 0.675, 0.7, 0.725, 0.75, 0.775, 0.8, 0.825, 0.85]$. For this numerical example the free design parameters for the cost function were set as $\alpha = 0.01$ and $\beta = 0.99$, while the forgetting factor λ was chosen to be 0. In this measurement data, the roll angle was obtained from spring displacement sensors, which measure the vertical travel of the suspensions. Despite the significant offset in roll angle measurement as noticeable from Fig. 20, the estimation results were successful.

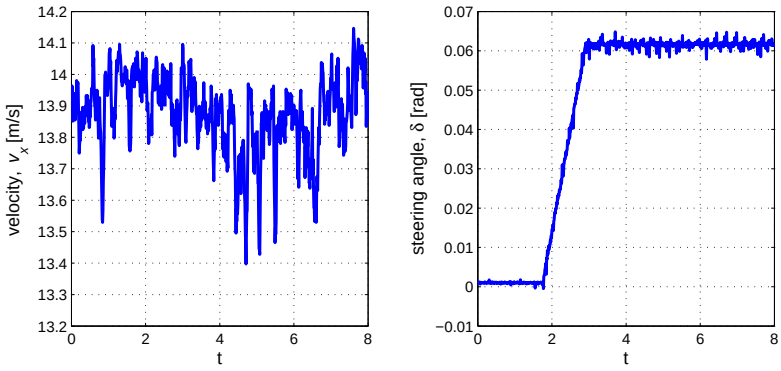

Figure 17. Velocity and steering angle inputs.

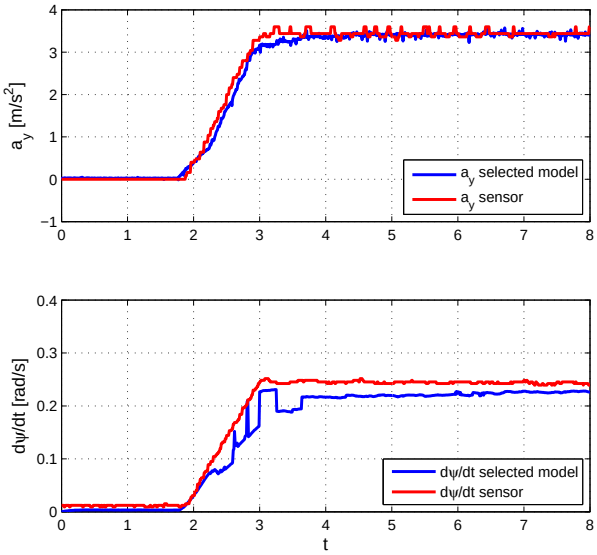

Figure 18. Comparison of the estimated and measured lateral acceleration and yaw rate.

Comment: It is important to note here that the specific problem at hand is about the estimation of unknown vehicle parameters in real-time rather than the control of specific vehicle states. Therefore, the abrupt switching between models and the corresponding "chattering" behavior in the estimations during the transient phase of the maneuvers is acceptable.

5 An application example: load condition estimator

In this section we introduce a problem related to rollover prevention for implementing our estimation technique. The problem originates from a particular robust rollover controller design in an SUV class vehicle such that when the vehicle is empty excluding the weight of driver, there is no risk of un-tripped rollover. In this case, a possible intervention of the controller results in a loss of performance and must be avoided. In what follows, we give a version of the multiple model & switching algorithm to estimate whether the load condition of the vehicle is above the threshold weight. The threshold weight here is defined by the total weight of the empty vehicle and the driver. For this problem we employed the roll plane model (10) and further assumed the availability of the set of the roll angle (ϕ), and the lateral acceleration (a_y) sensors. We also assumed that we know the parameters of the vehicle

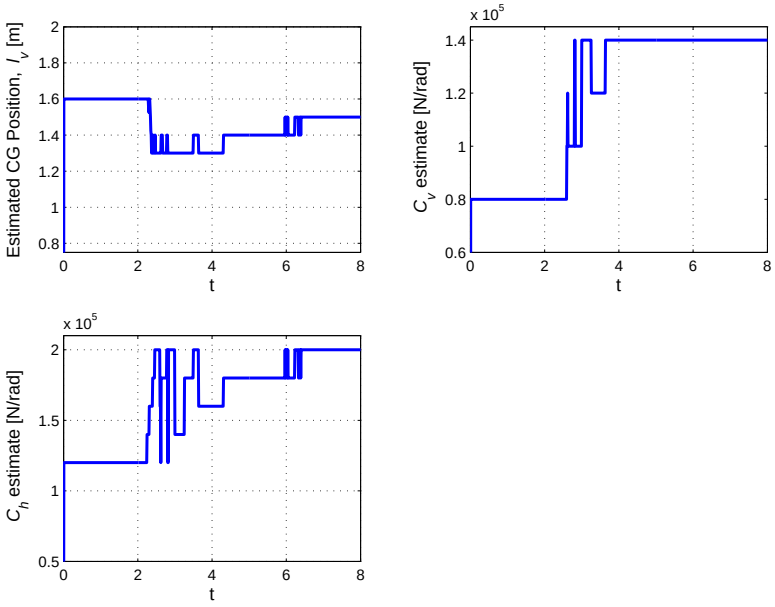

Figure 19. Estimations of longitudinal CG position and the linear tire stifnesses.

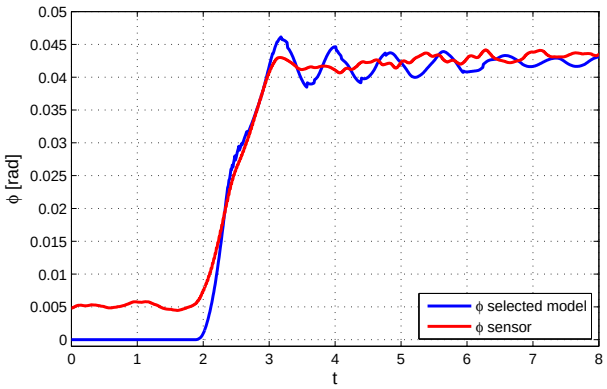

Figure 20. Roll angle measurement compared to the corresponding multiple model output.

corresponding to the threshold loading condition.

For the multiple model switching algorithm we set the known mass m, CG height h, damping coefficient c, and roll moment of inertia J_{xx} corresponding to the threshold loading condition to be the same in every model, where the models are parameterized with different spring stiffnesses. We assumed that spring stiffness belongs to a closed interval such that $k \in \mathscr{K}$, where the interval is divided into n grid points such that $\mathscr{K} = \{k_1, k_2, k_3, \ldots, k_n\}$. In other words we have n different models corresponding to the different k values. The equations of motion for the models with zero initial conditions can be expressed with (20). While each model is driven by the same input a_y, the corresponding identification errors e_i are calculated according to (21). Given this setup, one can compute cost functions (17) corresponding to each identification error and switching among the models based on (18) yields the one with the minimum cumulative identification error. The selected $k^\star$ represents the plant in the parameter space $\mathscr{K}$, and if it is different than that of the vehicle with threshold load condition then we can conclude that there is more load on the vehicle than the threshold value.

Numerical Analysis: In our simulations we chose the parameters given in Table 2 to represent the threshold loading of the vehicle. We also used the same obstacle avoidance maneuver introduced in the preceding section,

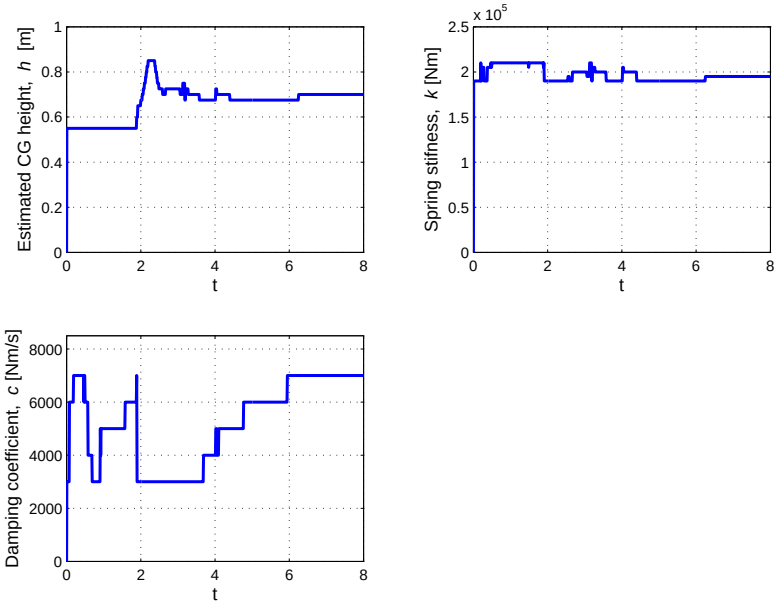

Figure 21. Estimations of CG height and the suspension parameters.

Table 3. Loading Scenarios

Case	Weight [kg]	CG height [m]	Threshold Loading?
1	**1300**	**0.70**	**yes**
2	1350	0.70	no
3	1400	0.70	no
4	1450	0.70	no
5	1500	0.70	no
6	1300	0.75	no
7	1300	0.80	no
8	1300	0.85	no
9	1300	0.90	no

at the speed of $108km/h$ and with a steering profile as shown in Fig. 6. We tested 9 different loading scenarios as described in Table 3, where the first case corresponds to the threshold loading condition. The model space consisted of 11 models in total, where the uniformly distributed parameter space was chosen as $\mathscr{K} = [30000, 40000]$ with intervals of 1000. Based on the described algorithm, only the first case was recognized as the threshold loading condition, and the recognition took less then 1.5 seconds into the maneuver in all the cases.

Based on the results, we conclude that this version of the multiple model & switching algorithm can successfully be used to rapidly recognize a specific loading condition of the vehicle based on the dynamics of the car alone, and utilizing only a small number of models.

6 Conclusions and discussions

In this paper we have presented a realtime parameter estimation algorithm using a multiple model switching approach incorporating simple linear models. Based on the simulation results, we demonstrated the accuracy of the suggested technique as compared to the traditional least squares identification approach, which shows significant benefits. We also presented preliminary tests of the algorithm with off-line measurement data taken from an undisclosed test vehicle, and results were promising. The results showed that the algorithm can also work in cases where the signals are corrupted by noise and bias. Moreover, the load condition estimator example demonstrated that a

simple version of the suggested algorithm can easily be integrated into current rollover or lateral dynamics controllers to enhance their performance.

Although the use of linear models in this analysis may be too restrictive for representing vehicle behavior, especially during extreme maneuvers, the method produced acceptable performance in the majority of the numerical tests. Exploration of more sophisticated and accurate nonlinear models, which are valid both in linear and nonlinear regions of operating regime, in conjunction with the multiple model approach shall be a future direction for research. In the follow-up of this work we shall also compare our estimation technique with nonlinear methods such as instrumental-variable type estimators to fully asses its potential, as these methods are more suited to the nonlinear parameter estimation task described in this paper, unlike the recursive least squares algorithm. In addition, we shall look into adaptive versions of the multiple model algorithm to deal with the cases when the parameter sets do not include the exact vehicle parameterizations. One important observation in our analysis was that the multiple model algorithm employing only fixed models required too many models to produce the desired estimation accuracy and performance (as apparent from numerical simulations where we had 140 models for lateral dynamics and 240 models for roll dynamics). This many models can cause a significant computational overhead for the current on-board computers used in cars. In order to remedy this problem, adaptive model space distribution techniques can be used, which employ only a small number of models initially and are updated and re-parameterized in fixed time intervals: this we shall exploit in our future work. Another direction for research shall look into integration of the algorithm with direct rollover prevention as well as lateral dynamics controllers and compare their feedback performance to that of alternative robust control approaches. We also aim for implementing the algorithm in a real vehicle and do extensive tests to asses the real-time performance as well as to determine the robustness of the algorithm to sensor uncertainties and/or other real life complications.

Comment: In the context of rollover mitigation control design, the CG height is an important parameter. We can demonstrate this by defining a non-dimensional parameter known as the load transfer ratio (LTR), which is obtained by a torque balance in the roll plane of the vehicle model given in Fig. 2. Based on this model LTR can be defined simply as follows

$$LTR = \frac{\text{Load on Right Tires-Load on Left Tires}}{\text{Total Load on All Tires}}. \tag{30}$$

It is evident that this parameter varies in the interval $[-1,1]$, and during straight driving for a perfectly symmetric car it is 0. The extremum is reached in the case of a wheel lift-off of one side of the vehicle, in which case it becomes 1 or -1. Therefore, a direct measurement or an estimation of this parameter can be used as a rollover warning, or as a switch for a rollover controller. Indeed LTR appeared previously in literature in a number of rollover prevention controller designs, most notably in [15] and [19], for assessing the rollover threat. A steady state approximation of LTR in terms of lateral acceleration a_y and the CG height h, as described in [15], is given below

$$LTR \approx \frac{2a_y}{g}\frac{h}{T}. \tag{31}$$

From this approximation the dependence of LTR, thus the rollover threat to the vehicle parameters a_y/g and h/T is apparent. Note that $\frac{a_y}{gT}$ can be measured whereas h is an unknown vehicle parameter. As apparent from (31), CG height is a prominent factor affecting rollover tendency of a vehicle, yet it is **not measurable**. Therefore any rollover mitigation controller can greatly benefit from the estimation of this specific parameter by tuning of the control parameters based on the estimated CG height. This in turn can significantly improve the lateral and the cornering performance of the vehicle in extreme driving situations without sacrificing its safety and handling capability. In the follow up of the current paper, we shall report a successful utilization of LTR parameter for rollover mitigation controller design, which incorporates the CG position estimation method described in this paper.

7 Acknowledgements

This work was supported by Science Foundation Ireland Grant 04/IN3/I478. Science Foundation Ireland is not responsible for any use of data appearing in this publication. The authors would like to thank Mr. Avshalom Suissa, and all the anonymous reviewers for their helpful comments and suggestions.

References

[1] National Highway Trafic Safety Administration (NHTSA), 2006, *Trafic Safety Facts 2004: A Compilation of Motor Vehicle Crash Data from the Fatality Analysis Reporting System and the General Estimates System*, Technical Report.
[2] Hac A., Brown T. and Martens J., 2004, Detection of Vehicle Rollover. *Vehicle Dynamics & Simulation*, SAE Technical Paper Series.
[3] Carlson C.R. and Gerdes J.C., 2003, Optimal Rollover Prevention with Steer by Wire and Differential Braking. *Proceedings of IMECE*, Nov. 16-21, Washington D.C. USA.
[4] Narendra K.S. and Balakrishnan J., 1993, Improving Transient Response of Adaptive Control Systems using Multiple Models and Switching. *Proceedings of the* 32nd *Conference on Decision and Control*, San Antonio, Texas.
[5] Narendra K.S. and Balakrishnan J., 1994, Improving Transient Response of Adaptive Control Systems using Multiple Models and Switching. *IEEE Transactions on Automatic Control*, Vol. 39, No. 9.
[6] Narendra K.S., Balakrishnan J. and Ciliz K., 1995, Adaptation and Learning Using Multiple Models, Switching and Tuning. *IEEE Control Systems*, No. 0272-1708/95.
[7] Akar M., Solmaz S. and Shorten R., 2006, Method for Determining the Center of Gravity for an Automotive Vehicle, Irish Patent.
[8] Mango N., 2004, Measurement & Calculation of Vehicle Center of Gravity Using Portable Wheel Scales. *SAE World Congress*, Mar. 8-11, Detroit, MI USA.
[9] Allen R.W., Klyde D.H., Rosenthal T.J., and Smith D.M., 2003, Estimation of Passenger Vehicle Inertial Properties and Their Effect on Stability and Handling. *Journal of Passenger Cars-Mechanical Systems*, Vol. 112.
[10] Vahidi A., Stefanopoulou A., and Peng H., 2005, Recursive Least Squares with Forgetting for Online Estimation of Vehicle Mass and Road Grade: Theory and Experiments. *Vehicle System Dynamics*, Vol.43, No.1 pp.31-55.
[11] Danish Ahmed, 2004, Parameter Estimation of Nonlinear Systems using an Extended Kalman Filter. *Diploma Thesis*, Technische Universität Kaiserslautern.
[12] Leimbach K.D., Wetzel G., 2006, Procedure and Device for Determining a Parameter Related to the Height of the Centre of Gravity of a Vehicle. *European Patent EP 0 918 003 B1*
[13] Chen B. and Peng H., 2001, Differential-Breaking-Based Rollover Prevention for Sport Utility Vehicles with Human-in-the-loop Evaluations. *Vehicle System Dynamics*, Vol.36, No.4-5, pp 359-389.
[14] Ackermann J. and Odenthal D., 1998, Robust steering control for active rollover avoidance of vehicles with elevated center of gravity. Proc. of International Conference on Advances in Vehicle Control and Safety, (Amiens, France).
[15] Odenthal D., Bünte T. and Ackermann J., 1999, Nonlinear steering and breaking control for vehicle rollover avoidance. European Control Conference, (Karlsruhe, Germany).
[16] Wielenga T.J., 1999, A Method for Reducing On-Road Rollovers: Anti -Rollover Braking. *SAE Paper* No. 1999-01-0123.
[17] Wielenga T.J. and Chace M.A., 2000, A Study of Rollover Prevention using Anti-Rollover Braking. *SAE Paper* No. 2000-01-1642.
[18] Palkovics L., Semsey À. and Gerum E., 1999, Roll-Over Prevention System for Commercial Vehicles-Additional Sensorless Function of the Electronic Brake System. *Vehicle System Dynamics*, Vol.4, pp.285-297.
[19] Kamnik R., Böttiger F., Hunt K., 2003, Roll Dynamics and Lateral Load Transfer Estimation in Articulated HeavyFreight Vehicles: A Simulation Study. *Proceedings of the Institution of Mechanical Engineers*, Part D.
[20] Schindler E., 2001, *Vehicle Dynamics*, Lecture notes, FHTE Esslingen University of Applied Sciences, Esslingen.
[21] Kiencke U. and Nielsen L., 2000, *Automotive Control Systems for Engine, Driveline and Vehicle*, (Springer-Verlag & SAE Int., Berlin).
[22] Van Zanten A., Erhardt R., Pfaff G., Kost F., Hartmann U. and Ehret T., 1996, Control Aspects of the Bosch-VDC. *AVEC'96 Int. Symposium on Advanced Vehicle Control*, Aachen, Germany.
[23] Abdellatif H., Heimann B., Hoffmann J., 2003, Nonlinear Identification of Vehicles Coupled Lateral and Roll Dynamics. *Proc. of the 11th IEEE Mediterranean Conference on Control and Automation*, Rhodes, Greece.
[24] Anton T. van Zanten, 2002, Evolution of Electronic Control Systems for Improving the Vehicle Dynamic Behavior. *AVEC'02 Int. Symposium on Advanced Vehicle Control*, Hiroshima, Japan.
[25] Söderström T., Stoica P., 1989, *System Identification*, Prentice Hall International, International Series in Systems and Control Engineering, (Cambridge, Great Britain).
[26] Àström K.J., Wittenmark B., 1995 *Adaptive Control*, 2nd edition, (Addison-Wesley Publ Co).
[27] Narendra K.S., Annaswamy A. M., 1989, *Stable Adaptive Systems*, (Prentice Hall International, Englewood Cliffs - NJ, U.S.A.).
[28] Narendra K.S., and Balakrishnan J., 1997, Adaptive Control using Multiple Models. *IEEE Transactions on Automatic Control*, Vol.42, No.2, pp 171-187.